Journal of Nanophotonics

Nanophotonics.SPIEDigitalLibrary.org

Designing nanostructured one-dimensional TiO_2 nanotube and TiO_2 nanoparticle multilayer composite film as photoanode in dye-sensitized solar cells to increase the charge collection efficiency

Jeganathan Akilavasan
Maufick Al-Jassim
Jayasundera Bandara

SPIE.

Designing nanostructured one-dimensional TiO_2 nanotube and TiO_2 nanoparticle multilayer composite film as photoanode in dye-sensitized solar cells to increase the charge collection efficiency

Jeganathan Akilavasan,[a] Maufick Al-Jassim,[b] and Jayasundera Bandara[a,*]
[a]Institute of Fundamental Studies, Hantana Road, Kandy CP20000, Sri Lanka
[b]NREL, 15013 Denver West Parkway, Golden, Colorado 80401, United States

Abstract. A photoanode consisting of hydrothermally synthesized TiO_2 nanotubes (TNT) and TiO_2 nanoparticles (TNP) was designed for efficient charge collection in dye-sensitized solar cells. TNT and TNP films were fabricated on a conductive glass substrate by using electrophoretic deposition and doctor-blade methods, respectively. The TNP, TNT, and TNT/TNP bi-layer electrodes exhibit solar cell efficiencies of 5.3, 7.4, and 9.2%, respectively. Solar cell performance results indicate a higher short-circuit current density (J_{sc}) for the TNT/TNP bi-layer electrode when compared to a TNT or TNP electrode alone. The open-circuit voltages (V_{oc}) of TNT/TNP and TNT electrodes are comparable while the V_{oc} of TNP electrode is inferior to that of the TNT/TNP electrode. Fill factors of TNT/TNP, TNT, and TNP electrodes also exhibit similar behaviors. The enhanced efficiency of the TNT/TNP bi-layer electrode is found to be mainly due to the enhancement of charge collection efficiency, which is confirmed by the charge transport parameters measured by electrochemical impedance spectroscopy (EIS). EIS analyses also revealed that the TNT/TNP incurs smaller charge transport resistances and longer electron life times when compared to those of TNT or TNP electrodes alone. It was demonstrated that the TNT/TNP bi-layer electrode can possess the advantages of both rapid electron transport rate and a high light scattering effect. [DOI: 10.1117/1.JNP.9.093091]

Keywords: 1-D TiO_2 nanotube structures; TiO_2 nanotube; dye sensitized solar cell; electron transport; scattering layer.

Paper 14093 received Sep. 5, 2014; accepted for publication Jan. 19, 2015; published online Feb. 20, 2015.

1 Introduction

TiO_2 nanotube arrays and their compositions are expected to exhibit improved and novel functional characteristics due to their higher surface area and highly ordered and new structures. In recent years, many one-dimensional (1-D) TiO_2 nanomaterials such as nanowires,[1] nanotubes,[2] and nanorods[3] have been synthesized by several methods and applied successfully, especially on the dye sensitized solar cells (DSSCs) fabrications. These 1-D structures provide direct and continuous pathways for electron transport from the injection points to the charge collection substrate enhancing the charge collection efficiency in DSSCs. However, much work has been focused on highly ordered TiO_2 nanotube arrays fabricated by anodization of titanium metal.[4,5] Use of TiO_2 nanotubes for fabrication of DSSC reduces the number of particle boundaries within the TiO_2 layer and consequently results in a reduction in charge recombination yielding the opportunity to fabricate better DSSC than using TNP. Despite the improved electron transport properties of TNT, the efficiency of a TNT-based DSSC is inferior to that of a TNP-based DSSC, which was mainly attributed to their low-specific surface area leading to poor dye loading.[6] Nevertheless, DSSCs have been successfully fabricated using highly ordered pristine

*Address all correspondence to: Jayasundera Bandara, E-amil: bandaraj@ifs.ac.lk, jayasundera@yahoo.com
1934-2608/2015/$25.00 © 2015 SPIE

TiO_2 nanotube arrays on florien doped tin oxide (FTO) glass and on Ti foil with an efficiency of 9.1% and 7.6%, respectively.[7,8] However, as mentioned earlier, the present efficiency of TiO_2 nanotube electrodes is not comparable with the efficiency of DSSCs fabricated with TiO_2 nanoparticles, hence further improvement of efficiency is very important as there is a high potential for TNT-based DSSC devices.

Recently, several methods have been attempted to increase the overall solar cell performance of TiO_2 nanotube-based electrodes by modifying the pristine TiO_2 nanotube structures. Out of the various methods employed to enhance the overall solar cell efficiency of TiO_2 nanotube-based electrodes, the use of composite systems was found to be the most successful method since the bi-layer structure provides a high surface area for excess dye loading and also an optimized microstructure for light harvesting, an excellent electron recombination resistance and fast electron transport.[9–12] Recent research articles by Chen et al.[13] and Qiu et al.[14] discussed the details of the application of bilayer structures in DSSC. One such approach was the incorporation of a carbon nanotube (CNT) in the TiO_2 nanotube array in order to enhance the short-circuit current by enhancing the charge collection efficiency. A threefold enhancement in J_{sc} has been noted for a DSSC fabricated with a TiO_2 NT/CNT composite electrode.[15] In a similar approach, an enhancement in J_{sc} and hence the overall efficiency was reported after coating a thin ZnO film or ZnO rod-like nanostructures on a TiO_2 nanotube which provided a higher specific surface area for dye adsorption and suppressed the recombination of photo-induced electrons at the electrode/electrolyte interface.[16] Also, by mixing TiO_2 nanoparticles with nanotube clusters, an increase in efficiency has been noted due to the enhancement in dye adsorption and ionic transport of electrolytes.[17] On the other hand, the surface passivation of TiO_2 nanotube photoelectrodes has been widely used to improve the performance of dye-sensitized solar cells and enhanced efficiencies have been reported with both organic and inorganic materials as a surface-passivation layer. A higher open circuit voltage has been reported with surface passivation with inorganic materials such as MgO,[18,19] and $SrTiO_3$,[20] while enhanced photocurrents have been reported with organic passivation materials such as $PC_{61}BM$.[21,22] In an earlier publication, we noticed 10% and 50% increases in solar cell performance by treating a TiO_2 nanotube with 0.04 and 0.5 M $TiCl_4$, respectively.[23,24] In another approach, the infiltration of TiO_2 nanotubes with TiO_2 nanoparticles has been successfully employed by combining the merits of the NP's high dye loading and high light harvesting capability with the NT's straight carrier transport path and high electron collection efficiency to improve the DSSC performance.[25,26] In a recent study, enhanced solar cell efficiency has been achieved with the incorporation of multiwall carbon nanotube in a TiO_2 nanowire.[15]

Even though several composite methods have been tested for the enhancement of the solar cell performance of a TiO_2 nanotube photoelectrode, the TiO_2 nanotube-based photoelectrode solar cell could not achieve a comparable solar cell performance to that of TiO_2 nanoparticles. In a recent study, a promising bi-layer design with 1-D and 0-D TiO_2 nanostructures has been proposed and in one of the bi-layer designs, TiO_2 nanoparticles were solely employed as the dye adsorption layer while in the other study, they were employed as a light scattering layer as well.[27,28] A remarkable enhancement in solar cell efficiencies has been reported in either case, indicating that new 1-D/0D TiO_2 composites can represent a very versatile structure. Sun et.al prepared a photoanode consisting of an under layer of TiO_2 nanoparticles and an upper layer of TiO_2 nanotubes and achieved a power conversion efficiency of 8%. The enhanced efficiency was believed to be the result of rapid electron transport and the enhanced light-harvesting properties of the TNP-TNT structure.[29] In a very recent study, enhancement in incident photon-to-current conversion and light-harvesting efficiency was reported for a photoanode consisting of a highly ordered TNT array and a TNP scattering layer.[30] Similarly, an efficient DSSC with an enhanced short-circuit current due to high dye-loading and light-harvesting capability has been reported for a photoelectrode consisting of tri-layered 1-D, 3-D, and 0-D TiO_2 electrodes.[31]

Inspired by these reports where high specific surface area, long electron diffusion length, and enhanced light-scattering effect are the desired properties of a photoanode for an enhanced solar cell performance, in this report, we investigated a bi-layer photoelectrode consisting of a bottom layer of hydrothermally synthesized TiO_2 nanotube and an upper layer of TiO_2 nanoparticles on a TiO_2 nanotube layer. In the bi-layer structure, the TNP layer serves as both a light scattering layer as well as a dye adsorption layer while the TNT layer provides a long electron diffusion length. The solar cell performance of the bi-layer TNT-TNP electrode was correlated with the

light-scattering properties and electrochemical properties of photoelectrodes consisting of TiO_2 nanotube/TiO_2 nanoparticles to that of a TiO_2 nanotube and TiO_2 nanoparticle only.

2 Experimental

2.1 *Synthesis of TiO_2 Nanotubes and Preparation of Electrodes*

TNTs were synthesized via a hydrothermal process in which 2 g of TNPs (P25 Degussa, Germany) were well dispersed in 30 mL (two-thirds of the autoclave chamber volume) of 10 M NaOH aqueous solution by stirring for 1 h and then transferred into a Teflon lined autoclave followed by maintaining the chamber at 150°C for 48 h in a furnace. The hydrothermal product was washed with 0.1 M HCl solution and distilled water until the pH of the product reached 8.5. The TNT precipitate was suspended in water by ultra-sonication for 15 min at the operating power set to 45% using an ultrasonic horn homogenizer (BANDELIN SONOPULS HD 2200). TNTs were deposited on the blocking-layer (BL) coated conducting substrate via an electrophoretic deposition (EPD) method, in which a two-electrode system is utilized with a conducting substrate (F: SnO_2, sheet resistance 8 Ω/cm^2, Dyesol, Australia) as the anode and a Pt wire as the cathode. The electrolyte for EPD was prepared by mixing the TNT suspension and methanol in 2:1 (v/v) ratio. EPD was carried out at an optimized voltage of ~40 V for 10 min.[24] The deposited films were baked at 130°C for about 20 min and sintered at 500°C (ramp of 25°C/min.) for 45 min in a furnace. The TNT deposited photo-electrodes were treated with a solution of 0.5 M $TiCl_4$ which was prepared from the stock solution of 99.9% $TiCl_4$ (Sigma Aldrich). In order to treat the TNT photo-electrodes, 20 μL of 0.5 M $TiCl_4$ solution was dropped on the TNT films and kept in a petri dish for 30 min. After 30 min, the films were inclined to remove the excess $TiCl_4$ followed by air-drying. Finally, the post-treated TNT electrodes were sintered at 450°C for 45 min in a furnace.

TNPs-based electrodes were prepared by doctor blading the TiO_2 paste on the FTO substrate. The TiO_2 paste was prepared as follows. 200 mg of TiO_2 powder (P25 Degussa, Germany) was mixed well with Triton X 100 followed by adding 0.1 mL of acetic acid and then was ground well for about 20 min followed by the addition of ethanol to form a fine paste. The fine paste was applied on FTO substrates and the films were sintered at 450°C for 30 min (ramp of 25°C/min.). In order to prepare TNTs-TNPs composite-based photo-electrodes, the TNPs were coated onto the presintered and post-treated TNTs films by the doctor-blading method and sintering at 450°C for 30 min (ramp 25°C/ min). The thickness of the TNP layer on the TNT layer was varied by adding several tapes on the doctor-blading method. For dye loading, these electrodes were immersed in a dye solution containing 0.3 mM N719 (Dyesol, Australia) for 12 h and the electrodes were washed off with ethanol to remove the loosely bound dye molecules.

2.2 *Characterization of Photoelectrodes and Measurements of Solar Cell Parameters*

Scanning electron microscopy (SEM) (SEM, LEO 1530 Gemini field emission scanning electron microscope FE-SEM and Hitachi SU6000 FESEM) was used to characterize and study the surface morphology of an electrode. UV-vis absorbance spectra and diffuse reflectance spectra were measured using a Shimadzu 2450 UV-vis spectrophotometer. Voltage decay measurements were taken using a digital oscilloscope (Tektronix TDS 3032 B two-channel color digital phosphor oscilloscope). Electrochemical impedance spectroscopy (EIS) measurements and Mott–Schottky analysis were performed using Zahner Zennium Electrochemical Workstation. External quantum efficiency (EQE) measurements were performed on a Bentham PVE300 unit with TMc 300 monochromator. I-V measurements of the DSSCs were carried out under standard solar simulation (New Port AAA solar simulator) set to one sun illumination (100 mW/cm^2 at AM 1.5 G). The effective area of the solar cells for the I-V measurements was 0.25 cm^2. The intensity of light sources was calibrated using standard reference cells. The dye loading amount was calculated after desorbing the adsorbed dye on the TiO_2 electrodes in 3M methanol KOH solution and measuring the absorbance at a 550 nm wavelength.

3 Results and Discussion

The composite photoelectrode fabricated with a TNT bottom layer and a top TNP layer sensitized with Ru-dye showed an efficiency of 9.2%. The SEM images of bottom TNT and top TNP layers which were fabricated on FTO glass by simple electrophoretic and doctor blade methods, respectively, are shown in Figs. 1(a) and 1(c), respectively. The formation of nanotubes by hydrothermal treatment of TiO_2 nanoparticles has been demonstrated.[32] The characterization of TNT has been reported in our earlier publication.[23] The SEM image of partially formed TNT [Fig. 1(b)] films which were taken during hydrothermal process clearly shows the partially formed TiO_2 nanotube indicating the formation of TiO_2 nanotube from our synthesis. The SEM image of TNT reveals that the length and diameter of the hydrothermally synthesized titania nanotubes are ~250 and ~10 nm, respectively, and are deposited in a randomly oriented manner on FTO glass electrode. On the other hand, the TNP layer consists of TiO_2 nanoparticles with an average crystallite size of about 20 nm. The cross-sectional image of composite films of TNT/TNP on FTO glass shown in Fig. 1(d) indicates the photoelctrode consists of 5 and 10-μm thick TNT and TNP layers, respectively. A magnified cross-sectional image of the composite films of TNT/TNP shown in the inset in Fig. 1(d) indicated tightly packed TNT and mesoporous TNP layers. The crystal structure of the TNT/TNP on FTO glass was also characterized by means of x-ray diffraction (XRD). Figure 2 shows the XRD patterns of TNT and TNT/TNP films annealed in air at 500°C. The peaks at 25.3 deg and 27.4 deg are the characteristic reflection of anatase and rutile, respectively.[16] As shown in Fig. 2, TNT consists mainly of the anatase form of TiO_2 and both TNT and TNT/TNP films showed characteristic diffraction peaks at 2Θ of 25.36 (101), 37.36 (004), 48.58 (200), 53.6 (105), and 63.28 (204), corresponding to the anatase TiO_2 phase in agreement with the standard reported values (JCPDS 21-1272). In the case of TNT/TNP, additional peaks at 2Θ of 27.58 (110), 36.2 (101), and 51.66 (211) are clearly

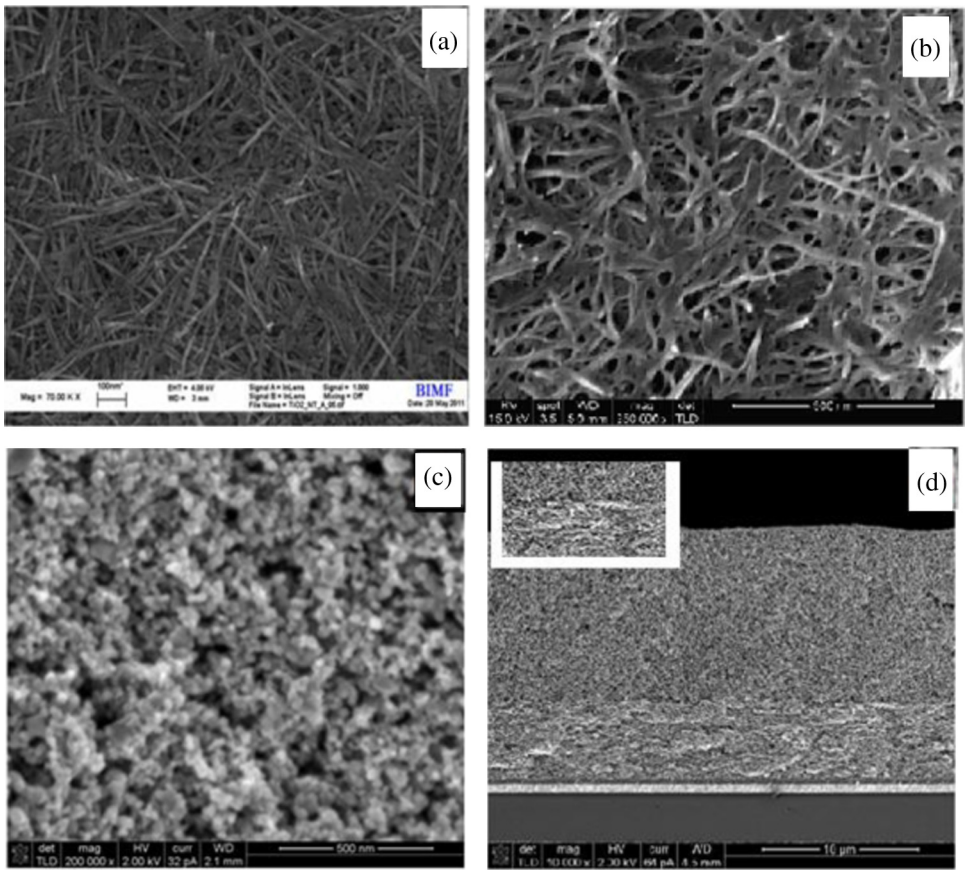

Fig. 1 SEM images of (a) bottom TNT layer, (b) partially formed TNT, (c) top TNP layers and (d) cross-sectional view of TNT/TNP electrodes which were fabricated on FTO glass by simple electrophoretic and doctor blade methods.

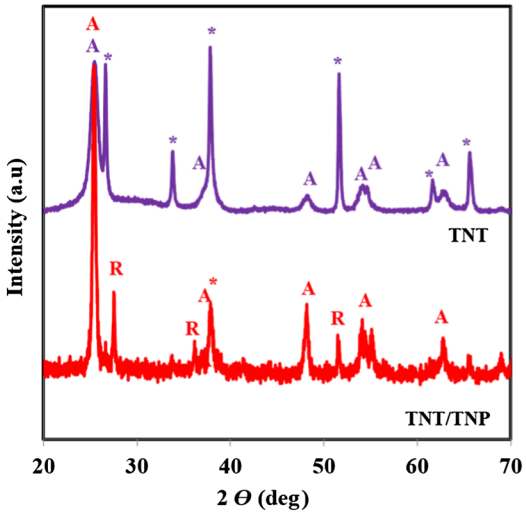

Fig. 2 X-ray diffraction (XRD) pattern of TNT and TNT/TNP films annealed in air at 500°C.

seen which are due to the rutile form of TiO_2 and correspond to the P25 Degussa TiO_2. The peak positions and their relative intensities are consistent with the standard powder diffraction patterns of anatase and rutile TiO_2. Note that the diffraction peaks with asterisks are due to the FTO substrate.

The current-voltage characteristics of the DSSCs based on TNT, TNP, and TNT/TNP electrodes sensitized with N719 dye with a liquid electrolyte of I^-/I_3^- under the AM 1.5 G illumination at a light intensity of 100 mW cm^{-2} are shown in Fig. 3 and the photovoltaic values are given in Table 1. As shown in Fig. 3(a), for the TNP electrode alone, the best solar cell performance was observed for a ~10 μm film and a J_{sc} of 13.8 mA/cm^2, a V_{oc} of 680 mV, an FF of 56.3%, and an η of 5.3% were observed. At the same time, for an optimized 5-μm thick TNT electrode alone, a J_{sc} of 14.2 mA/cm^2, a V_{oc} of 772.1 mV, an FF of 66.4%, and an η of 7.3% were shown. Interestingly, the optimized composite electrode consisting of a bottom TNT (5 μm) and a top TNP layer (10 μm) showed a record efficiency of 9.2% with a J_{sc} of 19.8 mA/cm^2, a V_{oc} of 749.2 mV, and an FF of 62.3%. However, when the thickness of the TNP layer decreases below 5 μm or increases over 15 to 25 μm, a decrease in J_{sc} was noted without a drastic change in V_{oc} and FF and a TNP layer thickness of ~8 to 12 μm showed an average efficiency of ~9.2%. The corresponding IPCE spectra of TNP, TNT, and TNP/TNP electrodes based DSSCs as a function of wavelength are shown in Fig. 3(b) and the IPCE values shown in Fig. 3(b) are also in good agreement with the observed J_{sc} of TNP, TNT and TNP/TNP electrodes shown in Fig. 3(a). The maximum peak of IPCE curves for all TNP, TNT and TNP/TNP electrodes based on DSSC exhibit at ~530 to 550 nm in the visible region and vary ~50%, 60%, and 70%, respectively. From the IV characteristics of TNP, TNT, and TNP/TNT, it is clear that the photoelectrode consisting of both TNP and TNT results in enhanced solar cell performance mainly due to enhancement in J_{sc}. Comparing the IV characteristics of individual TNT and TNP electrodes, it can be said that both electrodes showed similar J_{sc} values while TNT showed better V_{oc} and FF compared to TNP, yielding a higher solar cell performance for TNT-based electrode. The higher V_{oc} and FF of TNT-based electrode is a well-known fact and can be attributed to the 1-D nature of TNT structures leading to better electron transport and diminished charge recombination in 1-D-based solar cell devices.[3] As such, by combining TNP and TNT structures, we were able to achieve over a 9.2% solar cell efficiency for a DSSC which is ~26% and ~70% enhancement in overall solar cell efficiency compared to individual TNT and TNP-based electrodes, respectively. The overall enhancement of solar cell efficiency of TNT/TNP composite-based electrode could be due to several reasons such as enhanced light trapping due to better light scattering, enhanced charge collection, lifetime, and better diffusion of electrons as well as enhanced chemical capacitance of the composite films. We have investigated all these factors by EIS, reflectance spectra and Mott–Schottky methods in order to understand the higher solar cell efficiency of TNT/TNP composite films.

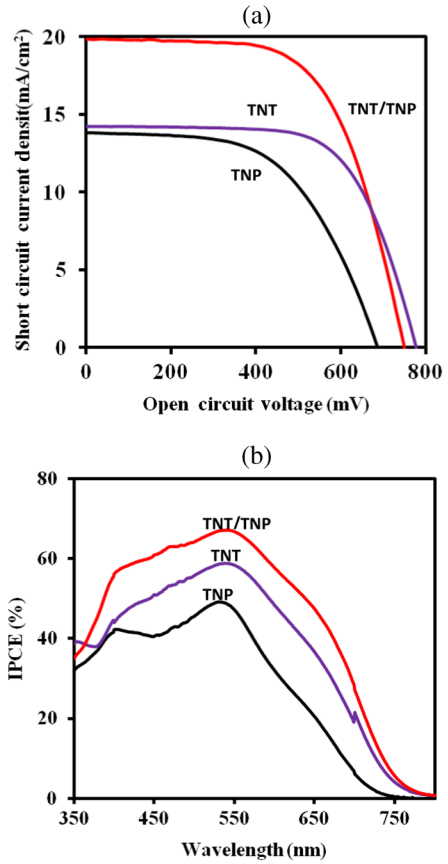

Fig. 3 (a) DSSC performance of TNP, TNT, and TNT/TNP-based electrodes at 100 mW/cm^2 irradiation at AM 1.5 G. (b) IPCE spectra of TNP, TNT, and TNT/TNP-based electrodes.

To understand the light scattering effect on J_{sc} and the overall solar cell performance, the following expression of dependence of J_{sc} on the light harvesting efficiency has been established:

$$J_{sc} = q n_{lh} n_{inj} n_{cc} I_0, \tag{1}$$

where q is the elementary charge, n_{lh} is the light harvesting efficiency of thin films and n_{inj} is the charge injection efficiency, n_{cc} is the charge collection efficiency, and I_o is the light intensity. The light harvesting efficiency n_{lh} is mainly determined by the adsorbed dye amount and the light scattering properties of the film, while light scattering has no effect on n_{inj} and n_{cc}. Dye adsorption results indicate more dye adsorption in the order TNP < TNT < TNT-TNP films, where the amount of dye coverage on TNP, TNT, and TNT-TNP films are 5.79×10^{-7}, 6.66×10^{-7} and 7.41×10^{-7} dye mol/cm^2, respectively, indicating that effective dye adsorption mainly originated from the TNT layer. A higher dye adsorption on TNP layer than the TNT layer of a bi-layer containing both TNP and TNT electrodes has been reported.[12] However, in the present investigation, we have noted enhanced dye adsorption on TNT rather than on the TNP layer

Table 1 DSSCs parameters of TNP, TNT, and TNT/TNP composite based electrodes at 100 mW/cm^2 irradiation at AM 1.5 G.

Cell	J_{sc} (mA/cm^2)	V_{oc} (mV)	FF (%)	η (%)
TNP	13.8	680.9	56.3	5.3
TNT-T	14.2	772.1	66.4	7.3
Composite	19.8	749.2	62.4	9.2

which could be due to the $TiCl_4$ treatment. If we compared the dye coverage's of TNT and TNT/TNP electrodes, 10% and 30% increases in dye adsorption in TNT/TNP over TNT and TNP, respectively, can be noted. Similarly, if J_{sc} of TNT, TNP and TNT/TNP are compared, 30% and 40% increases in J_{sc} for TNT/TNP compared to TNT and TNP alone, respectively, can be noted. Hence, it can be assumed that the observed higher J_{sc} for the composite TNT-TNP electrode may not be essentially due to dye coverage but could be due the light scattering effect.

To investigate the light scattering effect, diffuse reflectance measurements of TNP, TNT, and TNT/TNP films were carried out and we compared the light scattering properties of the TNT, TNP, and TNT/TNP films by normalized diffuse reflectance spectroscopy. It is interesting to note the extended visible light absorption especially in the TNT layer which we believe arises due to the formation of defect sites in TiO_2 owing to several quick-annealing processes during the thin-film preparation step.[33] As shown in Fig. 4, the light scattering of the TNP film was lower than both the TNT and TNT-TNP films, especially in the shorter wavelength regions, while a stronger light scattering was noted for TNP in the longer wavelength regions than TNT due to bigger TiO_2 particle aggregation. However, the TNT-TNP composite film showed enhanced reflectance over TNP in the whole spectrum region while the light reflectance of the TNT/TNP film is higher than TNT films only in the 500 to 300 nm region. The lower light reflectance of TNP films in the shorter wavelength regions can be understood on the basis that those uniformly stacked, mesoporous nanoparticles could not scatter light efficiently. On the other hand, the higher light scattering of TNT films is known and can be understood as randomly deposited TNT structures (SEM image, Fig. 1) allowing light to scatter efficiently. Interestingly, the higher light scattering effect of the composite TNT-TNP film could be assigned to both the higher light scattering of TNT and the infiltrated TNP in the TNT layer. As the light scattering effect is stronger in the TNT/TNP film than that of TNT or TNP alone, the enhanced light harvesting by TNT/TNP could lead to an increase in the photocurrent of the DSSCs. As such, due to highest adsorbed dye amount and the better light scattering effect of the TNT/TNP electrode than that of individual TNT or TNP electrodes, the observed highest quantum efficiency of the TNT/TNP electrode can be justified.

For further substantiation of the enhanced solar cell performance of the bi-layer TNT/TNP film, we investigated the electron transport properties of TNP, TNT, and TNT/TNP electrodes by EIS measurements. Impedance measurements of TiO_2 films were performed by applying a 10 mV AC signal over the frequency range of 0.1 Hz to 1 MHz under one sun illumination at different V_{oc}s. The Nyquist plots and Bode plots of these TiO_2 nanotube films of TNT, TNP, and TNT/TNP electrodes are shown in Figs. 5(a) and 5(b), respectively, which were fitted according to the equivalent circuit derived from the transmission line model of DSSCs. In the Nyquist plot shown in Fig. 5(a), only two semicircles were seen, where the semicircle at the high-frequency (10^6 to 10^3 Hz) is associated with the redox reaction I^-/I_3—at the Pt/electrolyte interface (R_{pt}), whereas the larger circle at the midfrequency (1 to 0.01 Hz) region is assigned to the electron transport (R_w) in the TiO_2 network and the electron transfer at the oxide/electrolyte

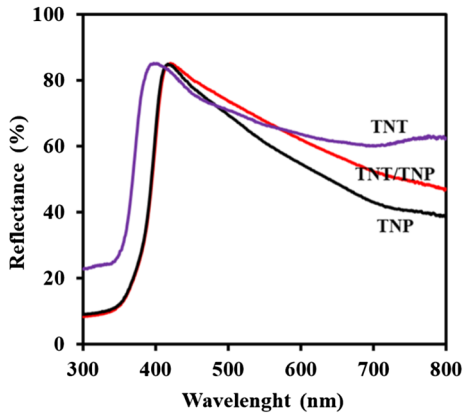

Fig. 4 Normalized diffuse reflectance spectra of TNP, TNT, and TNP/TNT films deposited on FTO.

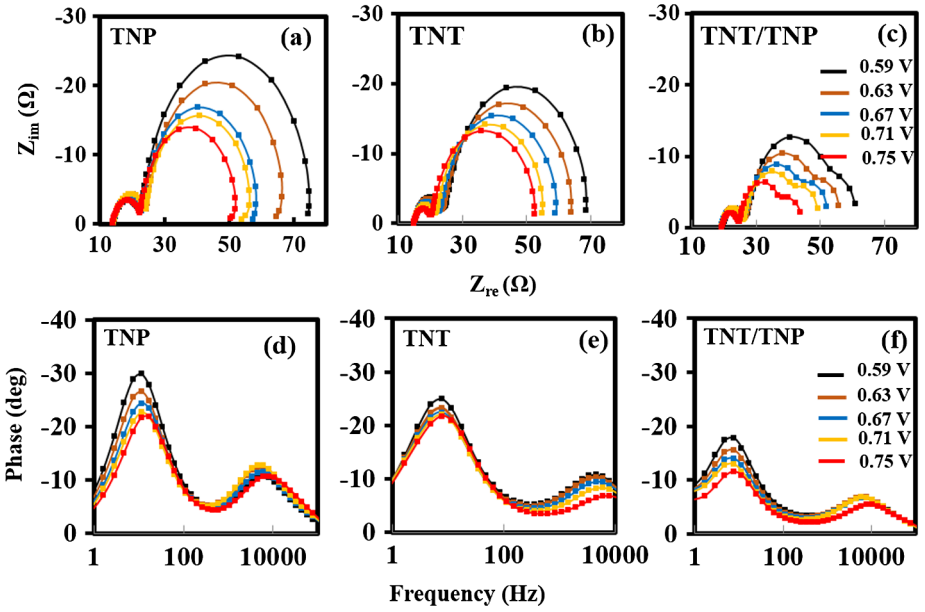

Fig. 5 EIS spectra (a)–(c) and respective Bode plots (d)–(f) of the DSSCs based on TNP, TNT, TNT/TNP electrodes respectively at various DC bias potentials.

interface (R_k) for the charge transfer processes occurring at the TiO_2/dye/electrolyte interfaces. The charge transport resistance (R_w) is overlapped with R_k in the semicircle at the midfrequency region due to the characteristic of $R_k \gg R_w$.[34]

The potential dependences of the transmission line parameters of R_k, R_t, τ_n and C_μ were extracted from the EIS fits and are shown in Fig. 6 and the calculated R_k, R_w, C_μ, and τ_n values at an applied potential bias at V_{oc} under 1 sun illumination are given in Table 2. By a simple comparison of the middle semicircles of the DSSCs shown in Fig. 5, a decrease in the diameter of the semicircle in the order TNT > TNP > TNT-TNP was noted, suggesting that the highest and lowest charge recombination resistance at the TiO_2/dye/electrolyte interface by TNT and TNT-

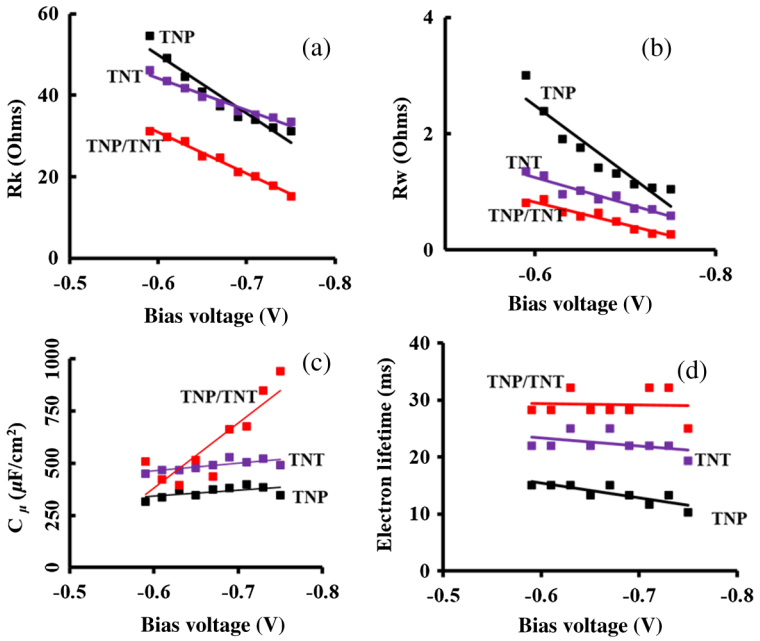

Fig. 6 (a) Recombination resistance, (b) charge transport resistance, (c) chemical capacitance, and (d) electron life time of DSSCs based on TNP, TNT, and TNT/TNP electrodes at various DC bias potential.

Table 2 EIS analysis results of DSSCs fabricated with TNP, TNT, TNT/TNP composite based electrodes.

EIS and phase at V_{oc} (−0.75) under illumination condition					
	R_k (Ω/0.25 cm^2)	R_w (Ω/0.25 cm^2)	τ (ms)	C_μ (μF/0.25 cm^2)	D_n (m^2/s)
TNP	31.18	1.04	10.34	347.4	2.9E – 07
TNT-T	33.45	0.59	19.04	489.8	1.04E – 07
Composite	15.22	0.27	24.96	939.6	6.13E – 07

TNP films, respectively. As shown in Fig. 6(a), the semi logarithmic plot of the recombination resistance (R_k) versus bias potential indicates the decrease of R_k with the increase of the forward bias for all TNT, TNP, and TNT-TNP electrodes. The potential dependence behavior of R_k which was determined in terms of the Buttler–Vollmer transfer factor similar to that explained by Fabregat-Santiago et al. was found to be the same for all three electrodes.[35] However, a lower R_k value is clearly seen for the TNT-TNP composite film compared to that of the TNT or TNP films. The calculated R_k values given in Table 2 confirm the lowest charge recombination resistance at the interface of TNT-TNP films and the highest charge recombination resistance for TNT films. The observed enhanced charge recombination at TNT-TNP films could be due to the higher surface area allowing facile transport of the redox couple in the TNT-TNP interface and thereby reducing the corresponding resistance at the interface.[36] The net result is a lower fill factor (FF) for the TNT-TNP-based electrode than the TNT-based electrodes. In fact, the solar cell performance given in Table 1 confirms the lower FF for the TNT-TNP-based electrode.

Though the charge recombination resistance of the TNT-TNP electrode is lower than that of the TNT electrode, the TNT-TNP-based electrode showed superior performance over that of the TNT or TNP-based electrodes. The superior solar cell performance of TNT/TNP electrode could be due to several other factors, such as better electron transport resistance, longer electron diffusion length, or higher electron diffusion coefficient, as well has higher chemical capacitance. As expected, the TNT-TNP composite film has a lower electron transport resistance, longer electron diffusion length, and higher electron diffusion coefficient, as well as chemical capacitance compared to TNT or TNP-based electrodes (Table 2). These factors may positively contribute to enhance the solar cell performance of the TNT-TNP-based electrodes as described below. If the behavior of the macroscopic charge transport resistance values of TNT, TNP, and TNT-TNP shown in Fig. 6(b) and Table 2 are considered, it is clear that at any given potential, TNT has a lower charge resistance than TNP. On the other hand, the lowering of R_w is noted in the case of the bi-layer TNT/TNP when the top layer of TNP is introduced on the bottom TNT layer. These results indicate that the electron transport in the TNT electrode is improved by mixing TNP with TNT, which could happen as some of the TNP may penetrate into the TNT structure enhancing the connectivity between TNTs. A better connectivity between TNTs in the TNT-TNP composite films could result in facile electron transport through the TNT network and thus, enhanced solar cell performance.

The other important parameter of photovoltaic operation is the capacitance behavior of the photoelectrode at the forward bias voltage. As shown in Fig. 6(c), the chemical capacitance of TNT, TNP, TNT-TNP electrodes increased with the increase of the bias voltage. The increase in capacitance is especially more dramatic for the composite film over that of the TNP or TNT electrodes. The increase in C_μ with the increase of the forward bias could be attributed to the increase in electron density (n) of the electrode due to dye injection raising the quasi-Fermi level (E_F) under illumination. As explained earlier, the C_μ of the device fabricated with TNT-TNP is higher than that of the TNT or TNP electrodes, indicating a higher electron concentration in the TNT-TNP composite electrode. A higher capacitance indicates a better electrical communication between the quasi-Fermi level in the semiconductor and the conducting substrate as a result of better interconnections of TNT-TNP. Additionally, the higher slope (α) of C_μ for the TNT-TNP electrode indicates a narrow distribution of the density of the trap states in TNT-TNP electrodes.[37] The narrow distribution of the trap states in TNT-TNP electrodes may

result in a negative shift in the flat-band potential leading to a higher V_{oc} of the device fabricated with the TNT-TNP electrode, hence, the observed higher V_{oc} for the composite TNT-TNP electrodes can be further justified. The other important parameter of photovoltaic operation is the electron lifetime (τ_n), which can be derived from the measured R_k, R_w and C_μ by EIS measurements. The τ_n under illumination is plotted against the applied bias voltage as given in Fig. 6(d). As shown in Fig. 6(d), τ_n ($\tau_n = R_k C_\mu$) decreases exponentially with the increase of the applied voltage. However, the electron lifetime observed for the TNT-TNP composite electrode is several times larger than that of TNT or TNP electrodes which suggests that the electrons injected from the excited dye to the TNT-TNP composite film can survive longer without undergoing losses at the bare FTO surface as well as in TNT nanostructures during charge collection. Hence, a higher solar cell performance can be expected for the TNT-TNP composite film than that of TNT or TNP electrodes.

In summary, the IV measurement results clearly demonstrated the enhanced solar cell performance of the composite bi-layer TNT-TNP anode over that of the individual TNT or TNP anodes and a record efficiency of 9.2% was reported for the composite anode film.

4 Conclusion

The photoelectrode consisting of a bottom TNT layer and a top TNP layer showed a record solar cell efficiency of 9.2%. Enhanced solar cell performance was found to be mainly due to the enhanced light scattering and better electron transport properties of the TNT/TNP composite films. Additionally, it was demonstrated that the composite films exhibit a higher chemical capacitance as well as longer electron lifetimes than that of individual TNT or TNP anodes. The addition of TNP in TNT may function as both a light scattering layer as well as connecting particles between the TNT nanostructures. The enhanced interconnected TNT may provide an uninterrupted electron path for injected electrons to be collected efficiently by the conducting substrate.

Acknowledgments

Financial support from NRC, Sri Lanka (NRC 2007-46) is highly appreciated.

References

1. J. Fan et al., "Enhanced photovoltaic performance of nanowire dye-sensitized solar cells based on coaxial TiO_2@TiO heterostructures with a cobalt(II/III) redox electrolyte," *ACS Appl. Mater. Interfaces* **5**(20), 9872–9877 (2013).
2. H. Park et al., "Fabrication of dye-sensitized solar cells by transplanting highly ordered TiO_2 nanotube arrays," *Sol. Energy Mater. Sol. Cells* **95**(1), 184–189 (2011).
3. B. Liu and E. S. Aydil, "Growth of oriented single-crystalline rutile TiO_2 nanorods on transparent conducting substrates for dye-sensitized solar cells," *J. Am. Chem. Soc.* **131**(11), 3985–3990 (2009).
4. K. Zhu et al., "Enhanced charge-collection efficiencies and light scattering in dye-sensitized solar cells using oriented TiO_2 nanotubes arrays," *Nano Lett.* **7**(1), 69–74 (2007).
5. J. R. Jennings et al., "Dye-sensitized solar cells based on oriented TiO_2 nanotube arrays: transport, trapping, and transfer of electrons," *J. Am. Chem. Soc.* **130**(40), 13364–13372 (2008).
6. K. Shankar et al., "Recent advances in the use of TiO_2 nanotube and nanowire arrays for oxidative photoelectrochemistry," *J. Phys. Chem. C* **113**(16), 6327–6359 (2009).
7. C.-J. Lin, W.-Y. Yu, and S.-H. Chien, "Transparent electrodes of ordered opened-end TiO_2-nanotube arrays for highly efficient dye-sensitized solar cells," *J. Mater. Chem.* **20**(6), 1073–1077 (2010).
8. L. Sun et al., "Conformal growth of anodic nanotubes for dye-sensitized solar cells: part I. planar electrode," *Nanosci. Nanotechnol. Lett.* **4**(5), 471–482 (2012).
9. L. Cao et al., "Double-layer structure photoanode with TiO_2 nanotubes and nanoparticles for dye-sensitized solar cells," *J. Am. Ceram. Soc.* **96**(2), 549–554 (2013).

10. K. Pan et al., "TiO_2-B nanobelt/anatase TiO_2 nanoparticle heterophase nanostructure fabricated by layer-by-layer assembly for high-efficiency dye-sensitized solar cells," *Electrochim. Acta* **88**, 263–269 (2013).
11. Q. Hu et al., "A novel TiO_2 nanowires/nanoparticles composite photoanode with SrO shell coating for high performance dye-sensitized solar cell," *J. Power Sources* **226**, 8–15 (2013).
12. H. Xu et al., "Enhanced efficiency in dye-sensitized solar cells based on TiO_2 nanocrystal/nanotube double-layered films," *Electrochim. Acta* **55**(7), 2280–2285 (2010).
13. H.-Y. Chen, D.-B. Kuang, and C.-Y. Su, "Hierarchically micro/nanostructured photoanode materials for dye-sensitized solar cells," *J. Mater. Chem.* **22**(31), 15475–15489 (2012).
14. Y. Qiu, W. Chen, and S. Yang, "Double-layered photoanodes from variable-size anatase TiO_2 nanospindles: a candidate for high-efficiency dye-sensitized solar cells," *Angew. Chem.* **122**(21), 3757–3761 (2010).
15. J. Y. Ahn et al., "Incorporation of multiwalled carbon nanotubes into TiO_2 nanowires for enhancing photovoltaic performance of dye-sensitized solar cells via highly efficient electron transfer," *Sol. Energy* **92**, 41–46 (2013).
16. S.-S. Kim, S.-I. Na, and Y.-C. Nah, "TiO_2 nanotubes decorated with ZnO rod-like nanostructures for efficient dye-sensitized solar cells," *Electrochim. Acta* **58**, 503–509 (2011).
17. X. D. Li et al., "Enhancing efficiency of dye-sensitized solar cells by combining use of TiO_2 nanotubes and nanoparticles," *Mater. Chem. Phys.* **124**(1), 179–183 (2010).
18. W. Sujuan et al., "Enhancement in dye-sensitized solar cells based on MgO-coated TiO_2 electrodes by reactive DC magnetron sputtering," *Nanotechnology* **19**(21), 215704 (2008).
19. P. Docampo et al., "Unraveling the function of an MgO interlayer in both electrolyte and solid-state SnO_2 based dye-sensitized solar cells," *J. Phys. Chem. C* **116**(43), 22840–22846 (2012).
20. S. Burnside et al., "Nanocrystalline mesoporous strontium titanate as photoelectrode material for photosensitized solar devices: increasing photovoltage through flatband potential engineering," *J. Phys. Chem. B* **103**(43), 9328–9332 (1999).
21. H. Park, C. Yang, and W.-Y. Choi, "Organic and inorganic surface passivations of TiO_2 nanotube arrays for dye-sensitized photoelectrodes," *J. Power Sources* **216**, 36–41 (2012).
22. J. Zhang, C. Tang, and J. H. Bang, "$CdS/TiO_2 - SrTiO_3$ heterostructure nanotube arrays for improved solar energy conversion efficiency," *Electrochem. Commun.* **12**(8), 1124–1128 (2010).
23. J. Akilavasan et al., "Significance of $TiCl_4$ post-treatment on the performance of hydrothermally synthesized titania nanotubes-based dye-sensitized solar cells," *Appl. Nanosci.* **4**(2), 185–188 (2014).
24. J. Akilavasan et al., "Hydrothermally synthesized titania nanotubes as a promising electron transport medium in dye sensitized solar cells exhibiting a record efficiency of 7.6% for 1-D based devices," *J. Mater. Chem. A* **1**(17), 5377–5385 (2013).
25. P. Xuan et al., "TiO_2 nanotubes infiltrated with nanoparticles for dye sensitized solar cells," *Nanotechnology* **22**(23), 235402 (2011).
26. Y. Alivov and Z. Y. Fan, "Efficiency of dye sensitized solar cells based on TiO_2 nanotubes filled with nanoparticles," *Appl. Phys. Lett.* **95**(6), 063504 (2009).
27. L. Zhao et al., "Double light-scattering layer film based on TiO_2 hollow spheres and TiO_2 nanosheets: improved efficiency in dye-sensitized solar cells," *J. Alloys Compd.* **575**(0), 168–173 (2013).
28. P. Roy et al., "Improved efficiency of TiO_2 nanotubes in dye sensitized solar cells by decoration with TiO_2 nanoparticles," *Electrochem. Commun.* **11**(5), 1001–1004 (2009).
29. K. C. Sun et al., "Enhanced power conversion efficiency of dye-sensitized solar cells using nanoparticle/nanotube double layered film," *J. Nanosci. Nanotechnol.* **13**(12), 7938–7943 (2013).
30. Z. He et al., "Double-layer electrode based on TiO_2 nanotubes arrays for enhancing photovoltaic properties in dye-sensitized solar cells," *ACS Appl. Mater. Interfaces* **5**(24), 12779–12783 (2013).
31. W.-Q. Wu et al., "Trilayered photoanode of TiO_2 nanoparticles on a 1D–3D nanostructured TiO_2-grown flexible Ti substrate for high-efficiency (9.1%) dye-sensitized solar cells with

unprecedentedly high photocurrent density," *J. Phys. Chem. C* **118** (30), 16426–16432 (2014).
32. H.-H. Ou and S.-L. Lo, "Review of titania nanotubes synthesized via the hydrothermal treatment: Fabrication, modification, and application," *Sep. Purif. Technol.* **58**(1), 179–191 (2007).
33. S. Kurian, H. Seo, and H. Jeon, "Significant enhancement in visible light absorption of TiO_2 nanotube arrays by surface band gap tuning," *J. Phys. Chem. C* **117**(33), 16811–16819 (2013).
34. T. Hoshikawa, R. Kikuchi, and K. Eguchi, "Impedance analysis for dye-sensitized solar cells with a reference electrode," *J. Electroanalyt. Chem.* **588**(1), 59–67 (2006).
35. F. Fabregat-Santiago et al., "Influence of electrolyte in transport and recombination in dye-sensitized solar cells studied by impedance spectroscopy," *Sol. Energy Mater. Sol. Cells* **87**(1–4), 117–131 (2005).
36. K.-M. Lee, V. Suryanarayanan, and K.-C. Ho, "The influence of surface morphology of TiO_2 coating on the performance of dye-sensitized solar cells," *Sol. Energy Mater. Sol. Cells* **90**(15), 2398–2404 (2006).
37. H. Wang et al., "Kinetics of electron recombination of dye-sensitized solar cells based on TiO_2 nanorod arrays sensitized with different dyes," *PCCP* **13**(38), 17359–17366 (2011).

Jeganathan Akilavasan is a PhD student in the nanostructures and optical materials research group at the Max-Planck-Institut für Kohlenforschung, Germany. He received his BSc in physical science and his MSc in nanoscience and nanotechnology from the University of Peradeniya, Sri Lanka, in 2008, and 2010, respectively.

Mowafak Al-Jassim is a principal scientist and group manager at the National Renewable Energy Laboratory. He received his PhD degree from the University of Oxford. He is the author of ~400 journal and conference papers. His current research interest includes the structural, morphological, luminescent, and electrical properties of photovoltaic materials and devices. His group develops and uses a wide variety of electron and scanning probe microscopy techniques for investigation defects and interfaces.

Jayasundera Bandara is a research professor, group leader of the photochemistry project at the Institute of Fundamental Studies, Sri Lanka. He received his PhD from EPFL, Switzerland, in 1998. His current research interests are synthesis of nanostructured materials and their applications in dye-sensitized solar cells and photocatalysis. He is the author of ~100 journal and conference research papers. He has been a reviewer and editorial board member for many internationally reputed journals.